Author's Accepted Manuscript

www.elsevier.com/locate/memsci

Desalination of seawater ion complexes by MFI-type zeolite membranes: temperature and long term stability

Bo Zhu, Zhou Hong, Nicholas Milne, Cara M. Doherty, Linda Zou, Y.S. Lin, Anita J. Hill, Xuehong Gu, Mikel Duke

PII: S0376-7388(13)00883-1
DOI: http://dx.doi.org/10.1016/j.memsci.2013.10.071
Reference: MEMSCI12514

To appear in: *Journal of Membrane Science*

Received date: 1 August 2013
Revised date: 30 October 2013
Accepted date: 30 October 2013

Cite this article as: Bo Zhu, Zhou Hong, Nicholas Milne, Cara M. Doherty, Linda Zou, Y.S. Lin, Anita J. Hill, Xuehong Gu, Mikel Duke, Desalination of seawater ion complexes by MFI-type zeolite membranes: temperature and long term stability, *Journal of Membrane Science,* http://dx.doi.org/10.1016/j.memsci.2013.10.071

Desalination of seawater ion complexes by MFI-type zeolite membranes: temperature and long term stability

Bo Zhu [a], Zhou Hong [b], Nicholas Milne [a], Cara M. Doherty [c], Linda Zou [d], Y.S. Lin [e], Anita J. Hill [c,f], Xuehong Gu [b] and Mikel Duke [a*]

[a] *Institute for Sustainability and Innovation, College of Engineering and Science, Victoria University, Werribee Campus, PO Box 14428, Melbourne, VIC 8001, Australia*

[b] *State Key Laboratory of Materials-Oriented Chemical Engineering, Nanjing University of Technology, Nanjing, Jiangsu 210009, P. R. China,*

[c] *CSIRO Materials Science and Engineering, Private Bag 10, Clayton South, VIC 3169, Australia*

[d] *Centre for Water Management & Reuse, University of South Australia, Adelaide, SA 5095, Australia*

[e] *School for Engineering of Matter, Transport and Energy, Arizona State University, Tempe, AZ 85287, USA*

[f] *CSIRO Process Science and Engineering, Private Bag 33, Clayton South, VIC 3169, Australia*

ABSTRACT

Ceramic membranes made from zeolites possess the nanoporous structure required for desalination of saline water including seawater. In this research, an α-Al_2O_3 supported MFI-type silicalite membrane was synthesised by the direct *in-situ* crystallisation method via a single hydrothermal treatment in an autoclave under autogenous pressure. Desalination performance of the prepared silicalite membrane was carried out with a seawater solution (0.3wt% TDS (total dissolved solids)) over a long period of around 180 days at a constant pressure of 700 kPa at various temperatures. The prepared silicalite membrane achieved a

* Corresponding author at: Institute for Sustainability and Innovation, College of Engineering and Science, Victoria University, PO Box 14428, Melbourne, Vic 8001, Australia. Tel: +61 3 9919 7682; fax: +61 3 9919 7696. Email: mikel.duke@vu.edu.au (M. Duke).

high rejection (>93%) for all major seawater ions including Na^+ (except for K^+, 83%) at an applied pressure of 700 kPa and room temperature (22 °C), but showed a continuous decrease in ion rejection when increasing the temperature from 22 °C and 90 °C. Permeation flux of the zeolite membrane significantly increased with increasing in temperature. Upon closer observation of the major cations, size selective diffusion in the zeolite membrane was observed over the temperatures tested. Larger ions Ca^{2+} and Mg^{2+} were less responsive to temperature than smaller ions Na^+ and K^+. No changes in membrane structure were observed by X-ray diffraction (XRD) and field emission scanning electron microscopy (FESEM) after 180 days seawater exposure. However, energy-dispersive X-ray spectroscopy (EDS) mapping on the surface of the membrane revealed a small quantity of tightly bound divalent cations present in the structure, which appear to have penetrated the zeolite, accelerated by temperature. They were suspected to have altered the permstructure, explaining why original high rejections at room temperature were not reversed after heat exposure. The work has shown that zeolite membranes can desalinate seawater, but other unusual effects such as ion selective diffusion as a function of temperature indicate a unique property for desalination membrane materials.

Keywords: Desalination; Seawater ions; Zeolite membrane; MFI; Silicalite

1. Introduction

Desalination is now commonly performed using membrane technology in reverse osmosis (RO) mode. However, the membrane types for desalination are limited to a handful of materials which imposes strict pretreatment requirements, such as chlorine/oxidant removal, abrasive particle removal and reduced operation temperature prior to feeding water to the polymer membrane. Also, the polymer material is subject to fouling which damages the membrane, either by the foulant itself, or the cleaning chemicals used to reverse the fouling [1]. Research and development in alternative membrane materials could enable more desalination opportunities where current membranes are limited. Harnessing inorganic materials for developing desalination membranes could be a more robust alternative relieving the costly pretreatment requirements required to conform to these material limitations.

The fundamental requirement of the membrane to carry out desalination by RO is an inherent ability of the membrane to repel ions, but pass water. High ion rejection properties

are essential in tandem with high water diffusion [2]. Nanoporous inorganic membranes have been studied both theoretically and experimentally to reject ions by filtration, utilising single layers [3] and a novel bilayer concept [4, 5]. Single layers are a more simplistic approach but the material must possess the required pore size between ions and the water. There have been some studies to date applying different membrane materials such as zeolites [2, 3, 6-10], and hybrid organically bridged silica [5] for membrane desalination. Zeolite materials are highly configurable through their chemistry and offer unique frameworks for a wide variety of applications including chemical sensing, water treatment and chemical reaction [2, 3, 6-13]. Their tuneable pore size, typically in the 0.3 to 1 nm range, makes them highly suitable for molecular sieving (i.e. ion rejecting) applications. Over the last decade, significant progress in the preparation and characterisation of zeolite membranes has stimulated research in their application for various molecular level separations including gas phase and liquid phase mixtures. Zeolites have also been shown to be outstanding candidate materials for desalination membranes as they possess the required small pore properties to reject ions [6, 10] as well as the thermal, chemical, and mechanical stability of ceramics [14].

A molecular dynamic simulation study conducted by Lin and Murad [10] showed that 100% rejection of Na^+ could be achieved using a perfect (single crystal), pure-silica ZK-4 zeolite membrane by RO. They found that zeolite pore structure is ideally suited to reject ions. The size exclusion of hydrated ions is the separation mechanism of the perfect ZK-4 zeolite membrane [15]. The aperture of the ZK-4 zeolite (diameter 0.42 nm) is significantly smaller than the kinetic sizes of hydrated ions (e.g. Na^+ 0.716 nm, K^+ 0.662 nm, Ca^{2+} 0.824 nm, Table 1) [16].

Table 1 Diameter of water and ions [17]

Ion	Hydrated diameter (nm)
H_2O	0.276
K	0.662
Cl	0.664
Na	0.716
Ca	0.824
Mg	0.856

Following this computational simulation study, several research groups have explored the possibility of using MFI-type zeolite membranes for desalination [2, 6-9]. The MFI-type zeolite has orthorhombic crystal symmetry with nearly cylindrical, 10-member ring channels. The aperture size of the MFI-type zeolite is around 0.56 nm [8], which is smaller than the sizes of hydrated ions [17] but larger than the kinetic diameter of water. Performance testing of MFI-type zeolite membranes working in RO demonstrated that high rejections of even the smallest ions, including Na^+ abundantly found in saline waters, are achievable [2, 6].

In general, permeation in an ideal molecular sieve zeolite membrane should occur only through the regular intracrystalline pores of the zeolite selective layer. In reality, however, the permeation properties will often be modified due to the existence of intercrystalline defect porosity caused by insufficient intergrowth of crystals, thermal removal of the template (e.g. tetra-propyl ammonium hydroxide (TPAOH)) [18, 19], or the complete de-watering of the membrane layer [20, 21]. Several researchers have reported changes in the unit cell dimensions of MFI-type zeolite crystals during heat treatment [21-24]. Our recent studies [25, 26] also showed that the interaction between MFI-type zeolites and the major cations in seawater causes changes not only in structure but also porosity, which is expected to affect diffusion properties of these materials when used as membranes for desalination. An easily modified feature of MFI-type zeolites is the Si/Al ratio which allows structures to be tailored to optimize the sorption uptake and species selectivity [27]. For example, increasing the content of alumina can alter properties such as surface hydrophobicity and surface charge which can have a significant impact on diffusion of electrolytes [27, 28]. Al-rich MFI-type zeolite (ZSM-5) membranes were recently reported to deliver higher water fluxes when compared with pure silica (silicalite-1) membranes using a pervaporation setup for desalination of NaCl solutions, but the silicalite-1 membrane exhibited relatively high robustness during a long term (560 h) stability testing [29]. Little work however exists on longer term (e.g. 180 days) performance of MFI-type zeolite membranes for reverse osmosis desalination of seawater ion complexes, or the performance as a function of temperature which may reveal unique diffusion effects through the dynamic zeolite cage and grain boundaries.

In this work, a MFI-type silicalite membrane was developed by a direct *in-situ* hydrothermal synthesis method. The as-synthesised zeolite membrane underwent long term (180 days) desalination of seawater ion complexes in the RO mode at different temperatures.

The structure and morphology of the zeolite membrane was also investigated by XRD and FESEM techniques.

2. Experimental and methods

2.1 Materials

1M TPAOH solution, sodium hydroxide pellets (NaOH, 99.99%) and fumed silica (SiO_2, 99.98%, particle size 0.014 µm, surface area 200±25 m^2g^{-1}) used for membrane preparation were purchased from Aldrich. The seawater solution (0.3wt% TDS) used for membrane desalination performance test was prepared from sea salts supplied by Sigma-Aldrich. All these chemicals were used as received without further purification. The porous α-Al_2O_3 disc shape support (99.8% Al_2O_3, ~27 mm diameter × 2 mm thick, average pore size of ~100 nm, ~30vol% porosity.) used for the current work was made by Nanjing University of Technology, China.

2.2 Membrane preparation

The MFI-type silicalite zeolite membrane was synthesised on the disk-shaped porous α-Al_2O_3 substrate by a direct *in-situ* crystallisation method via a standard hydrothermal process [2]. The synthesis precursor was prepared by dissolving 0.49 g NaOH pellets and 7 g fumed silica (99.98%, Aldrich) in 35 mL 1M TPAOH solution at 80 °C. The hydrothermal crystallisation process was conducted by placing the α-Al_2O_3 support into a Teflon lined stainless steel autoclave and adding the above prepared synthesis precursor solution and followed by hydrothermal treatment at 180 °C for 5 h. After hydrothermal synthesis, membrane was washed in deionised water to remove loose precipitate and was then calcined at 450 °C for 8 h with a heating/cooling rate of 1 °Cmin^{-1} to remove the organic template from the zeolite framework.

2.3 Membrane desalination

Desalination performance of the MFI-type silicalite membrane for a seawater solution (0.3wt% TDS) was carried out on the temperature-controlled membrane test rig (Fig. 1) at a pressure of 700 kPa and different temperatures (22 °C, 50 °C, 70 °C and 90 °C). The RO

experiments were conducted by a cross-flow operation with the membrane surface facing the feed solution and the substrate facing the permeate side. The membrane was first installed into the membrane cell and placed into the temperature control unit. The stainless steel feed vessel was charged with deionised water or 0.3wt% seawater solution. The operating pressure (700 kPa) was supplied by feeding N_2 into the feed vessel and was maintained constantly during the test. The cation concentrations of the collected permeate samples were analysed by inductively coupled plasma-optical emission spectrometry (ICP-OES) (PE Optima 4300 DV, Perkin Elmer instruments, USA) with 1500 w RF power. Rejection (r_j) of cation j was calculated by:

$$r_j(\%) = \frac{(c_{j,f} - c_{j,p})}{c_{j,f}} \times 100 \quad (1)$$

where $C_{j,f}$ and $C_{j,p}$ are ICP-OES measured concentrations of cation j (j = K^+, Na^+, Ca^{2+}, Mg^{2+}) in the feed and permeate solutions, respectively.

After desalination testing, the desalination system (including the membrane surface) was flushed with deionised water and the tested membrane was then oven dried for further characterisation.

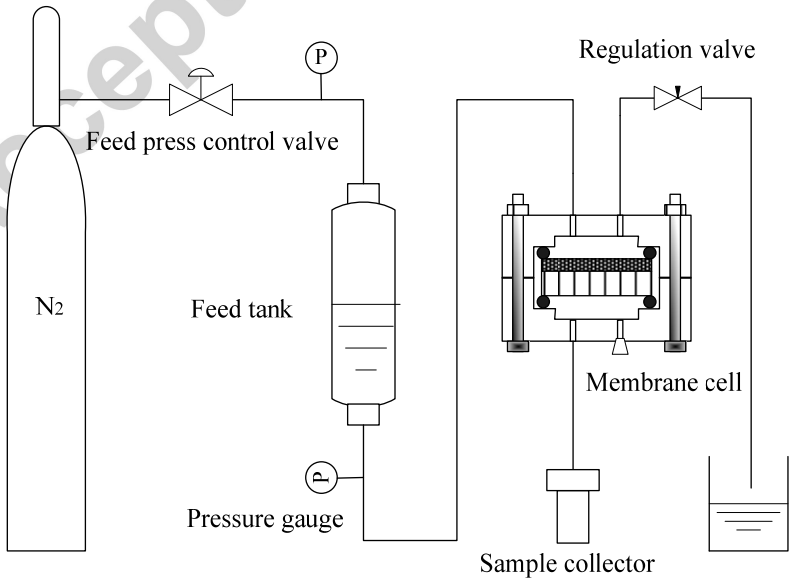

Fig. 1. Schematic drawing of the desalination system.

2.4 Characterisation

The original and desalination tested MFI-type silicalite membrane was characterised by XRD, SEM/EDS and single gas (He or N_2) permeation to determine any changes in membrane structure, morphology and surface elements after long term desalination testing at different temperatures. Prior to characterisation, the desalination tested membrane underwent deionised water permeation to remove weakly adsorbed material (including ions). The structure of the membrane was determined by XRD (D8-Advance, Bruker) and the XRD patterns showed no significant differences before and after long term seawater desalination testing. The textures of the membrane were observed by FESEM (S-4800, Hitachi) and the element analysis of the samples was carried out by EDS (Noran NSS 2.2, Thermo Scientific).

Positron annihilation lifetime spectroscopy (PALS) was used to investigate the effect of temperature on pore size of zeolites. Zeolite powders used for this study were prepared using the same procedures as used for the membrane preparation. PALS experiments were performed using an automated EG&G Ortec fast-fast coincidence system with fast plastic scintillators and a resolution function of 230 ps FWHM. To measure the long lifetimes, the range of the time-to-amplitude-converter (TAC) was extended to 200 ns and the coincidence unit was removed to improve the count rates. The 30 μCi ^{22}NaCl source was dried onto 2.54 μm thick Mylar film which required a source correction (1.605 ns, 2.969%). The original and seawater exposed zeolite powder samples were degassed at 150°C under vacuum for 16 hours prior to measurement. The positron source was sandwiched between 2 mm of powdered sample and evacuated to 5×10^{-7} Torr. A minimum of five spectra of 4.5 million integrated counts were collected per sample. The spectra were analyzed using LT9 software and were fitted to five components with τ_1 being fixed to 0.125 ns due to para-positron self-annihilation, and $\tau_2 \sim 0.35–0.45$ ns attributed to free positron annihilation. The average pore diameter for τ_3 was calculated using the Tao-Eldrup model assuming infinitely long cylindrical pore shape [30, 31]. The pore sizes for the long lifetimes (τ_4 and τ_5) were calculated using the rectangular Tao-Eldrup (RTE) model based on an infinitely long channel [32].

Gas permeation was conducted on a simple membrane test system with the same membrane cell used for desalination testing. The membrane was installed into the membrane cell and dried at 120 °C in the temperature control unit under N_2 prior to gas permeation testing. Permeation of either He or N_2 was carried out at 120 °C by feeding the gas at 100 kPa to the film-side of the membrane. The pressure decay occurred during the permeation test was monitored by a TPI 665 digital manometer (Test Products International, Inc. USA). The pressure was recorded by a computer with TPI 665 Data Logger software. Permeation was calculated by normalising the data to the membrane area and pressure drop.

3. Results and discussion

3.1 Desalination performance

The desalination performance of membrane was evaluated over 180 days of permeation at various temperatures from 22 °C to 90 °C. The membrane was tested with pure water (deionised water) for the first 10 hours, at which seawater was then introduced. The initial testing with pure water at room temperature (22 °C) showed a constant flux of ~0.03 $Lm^{-2}h^{-1}$. However, upon the introduction of seawater solution the permeate flux dropped by 33% to ~0.02 $Lm^{-2}h^{-1}$. The drop is related to the reduced driving force in overcoming the osmotic pressure determined by:

$$\pi = iMRT \qquad (2)$$

where π is the osmotic pressure (kPa), i is the van't Hoff factor of the solute (-), M is the molarity of the salt in solution, R is the universal gas constant (8.315 $LkPamol^{-1}K^{-1}$) and T is the system temperature (K). For binary salt solutions like NaCl (predominant in seawater), i is equal to 1.8 to represent incomplete dissociation (ion pairing). So the estimation of π in our experiment is 220 kPa. Since the membrane had high salt rejection (Fig. 4), the effect of osmotic pressure reduced the effective pressure by 32% correlating well with the observed flux reduction.

Figure 2 shows the specific flux which was estimated according to the following equations:

$$J_s = \frac{J}{p_{effective}} \quad (3)$$

$$p_{effective} = p_{total} - (\pi_{feed} - \pi_{permeate}) \quad (4)$$

where J_s ($Lm^{-2}h^{-1}kPa^{-1}$) is the specific flux, J ($Lm^{-2}h^{-1}$) is the flux obtained for a certain tested time and temperature, $p_{effective}$ is the effective pressure (kPa), p_{total} is the applied gauge pressure (700 kPa) when operating under ambient permeate pressures, and π_{feed} and $\pi_{permeate}$ are the osmotic pressure (kPa) calculated from Eq. (2) for the feed solution and permeate, respectively. It can be seen that the specific flux J_s was small ($<1.2\times10^{-4}$ $Lm^{-2}h^{-1}kPa^{-1}$) under an applied pressure of 700 kPa in all cases, being much smaller than state-of-the-art polymer membranes (estimated J_s $\sim40\times10^{-4}$ $Lm^{-2}h^{-1}kPa^{-1}$) used for seawater with a typical TDS of 35000 mgL^{-1} at operating pressures of 5.5–6.5 MPa to achieve water fluxes of 12–17 $Lm^{-2}h^{-1}$ [33]. While the flux achieved in this study is practically too low for industrial applications, we acknowledge that zeolite membranes synthesised by the in-situ method (thickness ~3 μm) [6, 7] are much thicker than commercial RO membranes (0.2 μm) [34, 35]. Membrane resistance to water transport is proportional to the dense skin thickness. As a result, water fluxes on polymer membranes are much higher than those through zeolite membranes.

Some simulation studies [36-39] have shown that a high pressure (e.g. 60–100 MPa) is required to infiltrate water into the purely siliceous pores of MFI zeolites (e.g. hydrophobic silicalite). However, a small increase in "hydrophilicity" of the porous framework could result in a change of the pores from being dry to being completely filled with water at saturation conditions [39]. It is known that during the synthesis of silicalite membranes, the alumina substrate will contribute some alumina into the zeolite thus departing it from ideal pure silicalite [40, 41]. Therefore, while we aim to make a silicalite membrane, we expect some alumina in our zeolite which makes it less hydrophobic thus providing more favourable conditions for water to enter the material.

Small fluxes have also been reported elsewhere for zeolite membranes [6, 42]. Kumakiri et al. [42] reported a total flux of 0.058 $Lm^{-2}h^{-1}$ (estimated J_s $\sim0.4\times10^{-4}$ $Lm^{-2}h^{-1}kPa^{-1}$) on a zeolite A membrane for RO mode rejection of ethanol from its aqueous solution under an applied pressure of 1.5 MPa. Li and co-workers [6] also reported a stabilised flux of

~0.112 $Lm^{-2}h^{-1}$ (estimated J_s ~0.6×10^{-4} $Lm^{-2}h^{-1}kPa^{-1}$) for a single 0.1 M NaCl feed solution under an applied pressure of 2.07 MPa and 0.058 $Lm^{-2}h^{-1}$ (estimated J_s ~0.4×10^{-4} $Lm^{-2}h^{-1}kPa^{-1}$) for a complex feed solution (0.1 M NaCl+0.1 M KCl+0.1 M NH_4Cl+0.1 M $CaCl_2$+0.1 M $MgCl_2$) under an applied pressure of 2.4 MPa with MFI-type zeolite membranes. Our recent study [43] on a MFI-type silicalite membrane prepared by the seeded secondary growth method also showed a flux of ~0.1 $Lm^{-2}h^{-1}$ (estimated J_s ~1.6×10^{-4} $Lm^{-2}h^{-1}kPa^{-1}$) for a 3000 mgL^{-1} (~0.05 M) NaCl feed solution under an applied pressure of 700 kPa. Therefore it seems the membrane used for this study exhibited reasonable fluxes under the pressure tested (700 kPa) as expected for zeolite membranes.

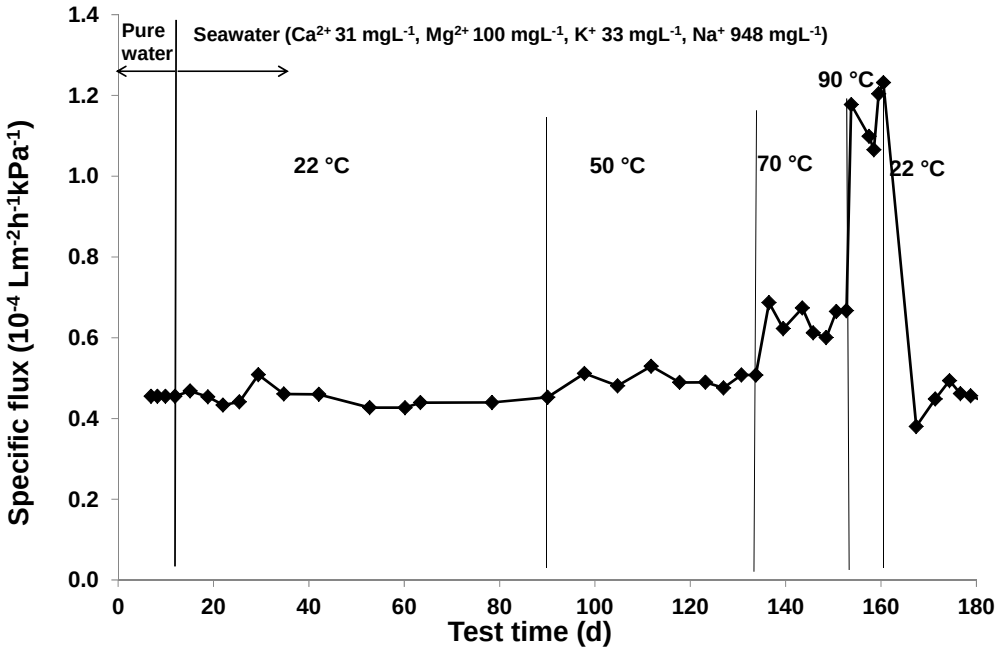

Fig.2. Variation of specific water flux on the MFI zeolite membrane with temperature during the long term desalination testing. Solution fed at 700 kPa pressure.

To reduce capital cost and increase desalination capacity, fluxes of zeolite membranes need to be significantly increased. While zeolite membrane thickness was mentioned as a potential reason for reduced flux, studies have shown that the flux of zeolite membranes could be improved by changing the hydrophobicity of the membrane [44] or through a single crystal zeolite nano-membrane [45]. Li et al. [46] decreased the hydrophobicity of the membrane by

adjusting the Si/Al ratio to 50 and increased the flux from ~0.11 $Lm^{-2}h^{-1}$ (estimated J_s ~0.4×10^{-4} $Lm^{-2}h^{-1}kPa^{-1}$) to ~1.1 $Lm^{-2}h^{-1}$ (estimated J_s ~4×10^{-4} $Lm^{-2}h^{-1}kPa^{-1}$) for a 0.1 M NaCl feed water under an applied pressure of 2.76 MPa. A most recent molecular dynamic stimulation study carried out by Liu et al. [45] showed that a nanoscale single crystal zeolite (FAU or MFI type) membrane with uniform pore size and high pore density can potentially achieve higher permeability (specific flux) than that of state-of-the-art polymer RO membranes. They also pointed out that for such zeolite nano-membranes to be suitable for practical desalination applications, the ratio of the membrane thickness to the pore radius of the porous substrate should be properly optimised. While flux optimisation is in need to meet expected fluxes of commercial polymer membranes, the key purpose of this work is to explore ion diffusion effects in high salt rejecting zeolite membranes.

The specific flux of seawater solution also remained almost constant for the whole testing period at room temperature (over 70 days at 22 °C), and showed a similar level to that of pure water (Fig. 2) confirming that the drop in flux upon the introduction of seawater solution after initial pure water test was caused by the decrease in the driving force (effective pressure) in overcoming the osmotic pressure. It was found from Figure 2 that there was only a slight increase in the specific flux when the operating temperature was increased to 50 °C, but a significant increase in specific flux was observed when temperature was further increased to 70 °C and 90 °C. The specific flux at higher temperatures (70 °C and 90 °C) was relatively unstable compared to that of lower temperatures (22 °C and 50 °C). The retesting at room temperature showed a similar level of specific flux to that between 22 °C and 50 °C.

It can be seen from Figure 2 that the specific flux increased at an increasing rate when the operating temperature increased from 22 °C to 90 °C (increased 2.5 fold). Increase in permeate flux with increasing temperature is typical for microprous materials, especially MFI-type zeolites as observed in pervaporation studies which is attributed to activated transport [29, 47]. In desalination through the same structures, activated diffusion was also observed by Li et al. [8]. They found in their study that both water and ion fluxes increased significantly when raising the feed temperature from 10 °C to 50 °C.

Changes in the absolute concentrations of cations in the permeate during the long term desalination testing were determined by ICP-OES and shown in Figure 3. The ion rejections calculated from the ICP-OES measured absolute concentrations by Eq. (1) are presented in

Figure 4. It was found from Figure 3 that some Na^+ and K^+ were detected in the permeate samples obtained from the initial pure water testing. Na^+ in the pure water permeate is likely due to the release of residual Na^+ from zeolite membrane preparation as NaOH was added in the synthesis precursor [6, 25]. During the preparation of the zeolite membrane with the high concentration of NaOH and SiO_2, significant amounts of Na^+ may have been trapped in the substrate and the zeolite intercrystal pores and formed some low-solubility sodium aluminosilicate compounds (e.g. Na_2SiO_3, $Na[Al(SiO_3)_2]$) during heat treatment [6]. These sodium aluminosilicate compounds cannot be thoroughly cleaned up by the regular rinsing and leaching processes but the Na^+ can dissolved slowly into the permeate solution during the RO operation [6]. The potassium ions present as impurities in the structure directing agent, TPAOH, are the source of K^+ detected in the pure water permeates. It is common in zeolite synthesis that Na^+ and K^+ impurities come from the commercially available TPAOH solutions [25, 48]. No Ca^{2+} and Mg^{2+} were detected in the permeates from the initial pure water testing as expected as there are no other sources of these ions other than what is provided in the seawater solution.

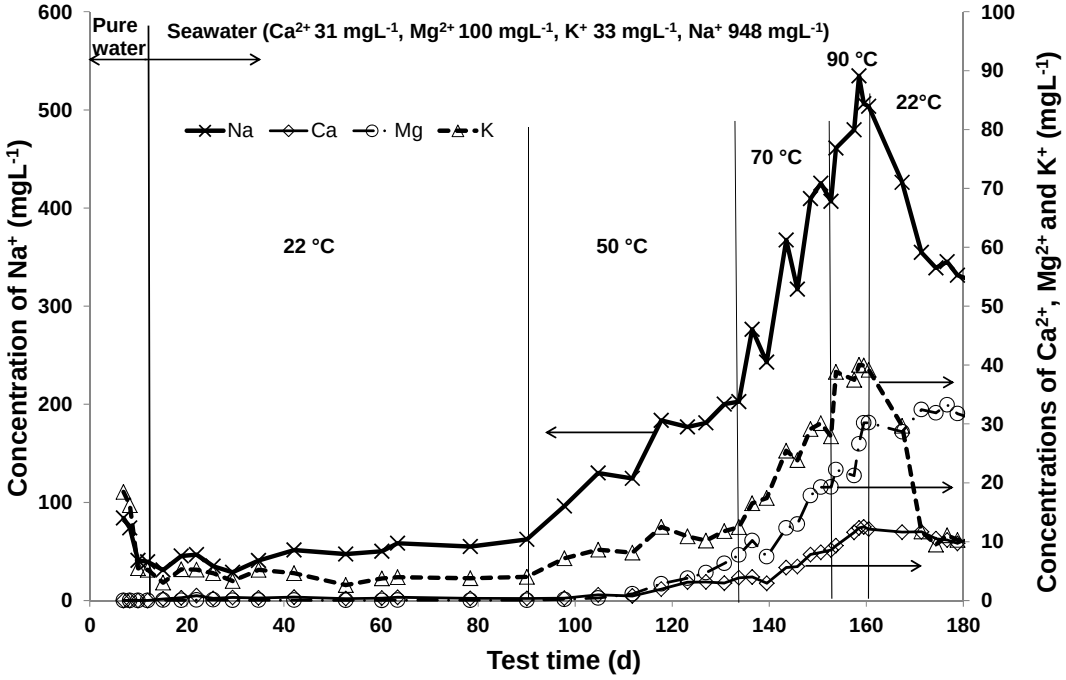

Fig.3. Concentrations of cations captured in the permeate samples obtained from the long term desalination testing on the MFI zeolite membrane. Solution fed at 700 kPa pressure.

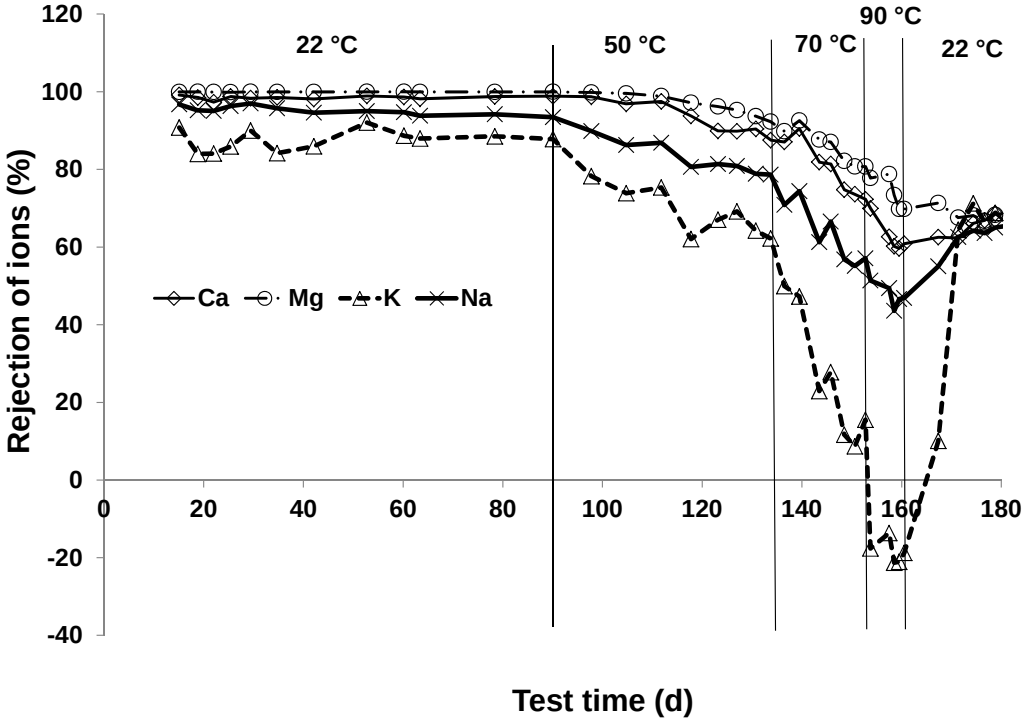

Fig.4. Ion rejections by the MFI zeolite membrane fed with 0.3wt% seawater solution (Ca^{2+} 31 mgL^{-1}, Mg^{2+} 100 mgL^{-1}, K^{+} 33 mgL^{-1}, Na^{+} 948 mgL^{-1}) at 700 kPa pressure.

With the introduction of 0.3 wt% seawater at room temperature (22 °C) there was almost no Ca^{2+} and Mg^{2+} measurable in the permeate samples (Fig. 3), indicating a high rejection for these cations (>98% for Ca^{2+} and >99% for Mg^{2+}, Fig. 4). Good rejections were also achieved for Na^{+} (>93%, Fig. 4) and K^{+} (>83%, Fig. 4) for this period of desalination, but they are not as high as those of Ca^{2+} and Mg^{2+}, indicating that the zeolite membrane is more favourable for the rejection of divalent cations Ca^{2+} and Mg^{2+} than monovalent Na^{+} and K^{+}. Similar trends were also observed in the study carried out by Li et al. [6] on the RO separation of the multiple-salt solution. Ca^{2+} and Mg^{2+} have higher ion charge density than Na^{+} and K^{+}, thus have greater ability to polarise the neighbouring water molecules and form larger and more rigid hydrated complexes [49, 50]. Na^{+} rejection of 93% achieved in the current work is the best RO desalination on MFI zeolite membranes shown so far at a low applied pressure of 700 KPa. Previous studies by Li and co-workers [6] showed a Na^{+} rejection of 76.7% for a single 0.1 M NaCl feed solution under an applied pressure of 2.07 MPa and 58.1% for a complex feed solution (0.1 M NaCl+0.1 M KCl+0.1 M

NH_4Cl+0.1 M $CaCl_2$+0.1 M $MgCl_2$) under an applied pressure of 2.4 MPa. More recently, Na^+ rejection (from 0.1M NaCl solution) was measured at 99.4% at 2.76 MPa [51]. Regardless, it is important to point out that MFI-type zeolites indeed have the required pore size to reject the most important ion, Na^+, from water thus making them suitable for water passive, ion rejective applications including desalination.

When the testing temperature was increased from 22 °C to 50 °C, there was an increase in permeate ion concentrations in all cases, with a significant increase being observed for Na^+ and K^+ (Fig. 3). As a consequence of this, the ion rejections decreased. However, the rejection for the divalent cations Ca^{2+} (>90%) and Mg^{2+} (>93%) still remained quite high compared to that of Na^+ (78–90%) and K^+ (60–80%) (Fig. 4). Further increase in operating temperature (70 °C to 90 °C) resulted in a significant increase in permeate ion concentrations in all cases (Fig. 3) thus leading to a significant drop in ion rejections (Fig. 4). As mentioned earlier, the permeate flux showed a significant increase when increasing the testing temperature to 90 °C. This affected both water and ions, but had a greater impact on the ion permeation than on the water permeation thus resulting in a decrease in ion rejection [8]. This is a special phenomenon which requires further exploration for specialist ion selective applications (e.g. nutrient recovery). It was also interesting to note that the rejections obtained for K^+ decreased to below 0% when the testing temperature was increased to 90 °C (Fig. 4). This unexpected observation of negative rejection of K^+ might be due to the piezodialysis [52] on the zeolite membrane. Piezodialysis is the mechanism of salt transport in preference to water, driven by pressure gradient. This would suggest that the zeolties can diffuse ions driven by pressure. It may be possible with potassium considering it is the smallest cation in solution and would presumably require transport of chloride anions to maintain charge neutrality in the permeate. However more data would be needed to prove our unexpected negative rejection to be piezodialysis within zeolites.

A combination of phenomena is likely to be responsible for the variation in rejection as a function of temperature witnessed here. As shown in Figure 5, the ion rejection increased with increasing hydrated diameter of ions (Table 1: $K^+ < Na^+ < Ca^{2+} < Mg^{2+}$) at all temperatures tested except for the retest at 22 °C after testing at 90 °C. These results have demonstrated a size selective diffusion in the RO process of the zeolite membrane. In particular it was found that there was a significant drop in rejection of the smallest of the hydrated cations K^+ as the operating temperature was increased. This is indicative of zeolite intrinsic pores opening in

the membrane to such an extent that the hydrated ion is easily accommodated in the structure and passage through the membrane becomes possible. Conveniently, the K^+ hydrated diameter is very close to that of Cl^-, being 0.662 nm and 0.664 nm respectively (Table 1). Charge balance can therefore be maintained by the simultaneous transfer of K^+ and Cl^-.

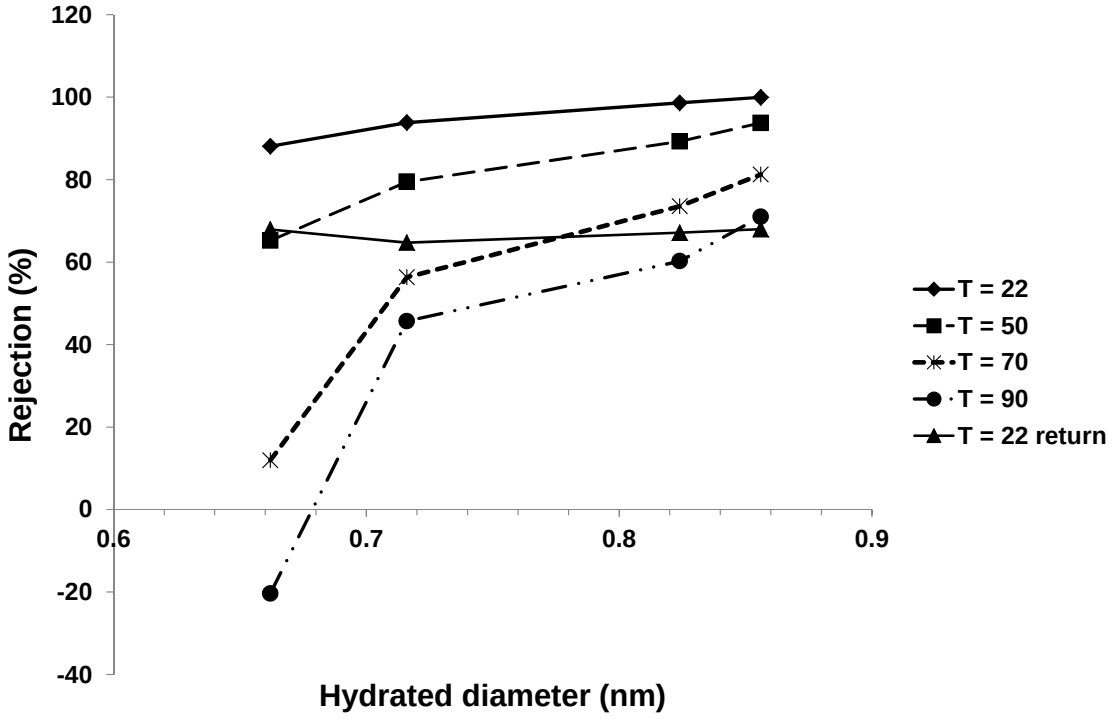

Fig.5. Ion rejections on a MFI zeolite membrane as functions of the hydrated diameter of ions (Table 1). 0.3wt% seawater solution (Ca^{2+} 31 mgL^{-1}, Mg^{2+} 100 mgL^{-1}, K^+ 33 mgL^{-1}, Na^+ 948 mgL^{-1}) fed at 700 kPa pressure and different temperatures.

In order to explore the overall effect of temperature on the intrinsic pores and grain boundaries, PALS was conducted with results shown in Figure 6. Temperature was observed to have a slight effect on pore size of the zeolite. As mentioned above, increasing temperature is known to increase the zeolite intrinsic pores as shown in the PALS result. However due to the large uncertainties calculated for each point, only a very general increasing trend can be shown. Uniquely at 90 °C, an intrinsic pore size of around 0.6 nm is possible within the upper limit of certainty. This is approaching the size of the hydrated Na^+ and Cl^-. Another interesting result from PALS showed that the microporous grain boundaries decreased in size

with increasing temperature, which may be due to the slight expansion of the crystals thus causing the boundaries to close. They are still large enough to accept all cations listed in Table 1 at 90 °C (>0.9 nm), but the effect of activated diffusion appeared to outweigh any size reduction. No significant trend was observed over uncertainties in size for the mesopores.

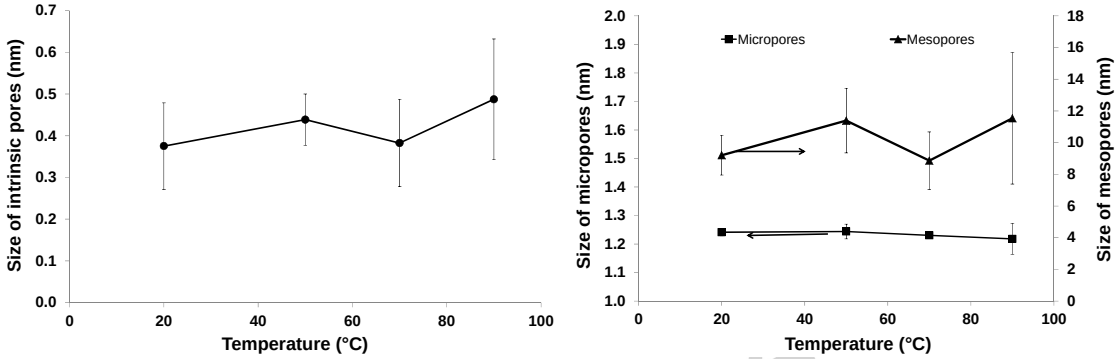

Fig.6. Effect of temperature on pore size of zeolites measured by PALS. Intrinsic zeolite pores (left) and non-zeolite pores (right) made of micropores and mesopores

It is also important to keep in mind that while the MFI structure is expanding with temperature, the extent of hydration of ions decreases [53]. This means that the hydration diameter decreases at the same time as the zeolite intrinsic pores open, leading to the breakthrough of the K^+ ion. Another important point is the slight changes in symmetry of the MFI structure that occurs throughout the temperature range being studied here. Early work into the MFI and ZSM-5 structures was able to show a symmetry change in the structure that occurs at 82–84 °C [54]. This slight, but distinct change may also contribute to a change in the pore characteristics of the structure, potentially enhancing diffusion or making the pores more accessible. If this is the case the reversibility of the system [55] would mean the structure would return on cooling, assuming no other changes have occurred.

Any charge-based rejection would also be reduced by the increased temperature. From a holistic viewpoint, the electrical double layer is the region where electrostatic forces of ordering outweigh the thermal forces of disorder [56]. From this concept, increasing the temperature would increase this disorder and weaken the effect of the double layer. This is

supported by theory that shows that while the characteristic thickness of diffuse layer would increase, the ability of the layer to store charge would decrease. This would allow more ready movement of ions near the surface of particles. In particular, this would influence diffusion via intercrystal pores where the double layer dominates ionic rejection mechanisms. This effect facilitates all ions, particularly the large divalents which cannot transport within the zeolitic pores, to diffuse through the membrane material.

The retest at 22 °C after testing at 90 °C showed a reversal in ion rejections to some extent, but did not achieve the similar level to that obtained for the initial test at 22 °C, suggesting that irreversible changes in the zeolite membrane might have occurred after testing at a relatively high temperature up to 90 °C. As was noted earlier, the change in symmetry in the MFI structure appears to be reversible suggesting this is not responsible for the change [55]. There is, however, an effect from the presence of different cations incorporated into the pores of the structure in order to maintain charge neutrality [55]. The reduction of the electrical double layer, enlargement of zeolite pores and increased rates of diffusion at higher temperatures have combined to allow not just significant transfer of K^+ to the permeate but also a rise in the transfer of other ions. This implies a greater incorporation of these ions in MFI. This is likely to be the source of the apparent irreversible change to the structure. Apart from the strong impact from the temperature, long periods (e.g.180 days) of desalination testing might also have led to some slight changes on the zeolite membrane although the structure was maintained at macroscale (Fig. 8b). The recent stability study carried out by Drobek, *et al.* [29] on zeolite membranes showed some permanent decay after up to 560 h desalination testing in pervaporation mode. This was due to the combined effects of ion exchange and water dissolution mechanisms.

3.2. Permeation activation energy

It is known that the ion flux can be described by the Arrhenius function and the permeation activation energy can be estimated from an Arrhenius plot. Figure 7 shows the Arrhenius plots for the cations Na^+, Ca^{2+}, and Mg^{2+}. We see for the points included in the plot, that they follow a linear relationship. The overall activation energies obtained for the cations are presented in Table 2. However it can be seen on Figure 7 that only the data obtained at 22 °C, 50 °C and 70 °C were used for K^+ as it deviated significantly when the temperature was over 70 °C. Due to the rapid increase in K^+ flux that is not attributed to conventional activated

transport (attributed to matching of zeolite pore size to hydration diameter), the data point for 70 °C begins to depart from the model for K^+ (Fig. 7) and the correlation coefficient R^2 for K^+ is lower than that for Na^+, Ca^{2+}, and Mg^{2+} (Table 2). As observed earlier, the pores appeared to open for K^+ (or its counter ion Cl^-) to penetrate freely through the material which would impact the diffusivity coefficient. Diffusion would require another relationship reflecting the dynamic structure of the zeolite, but interestingly we observe this is not significant until a certain point where a major change to diffusion is observed.

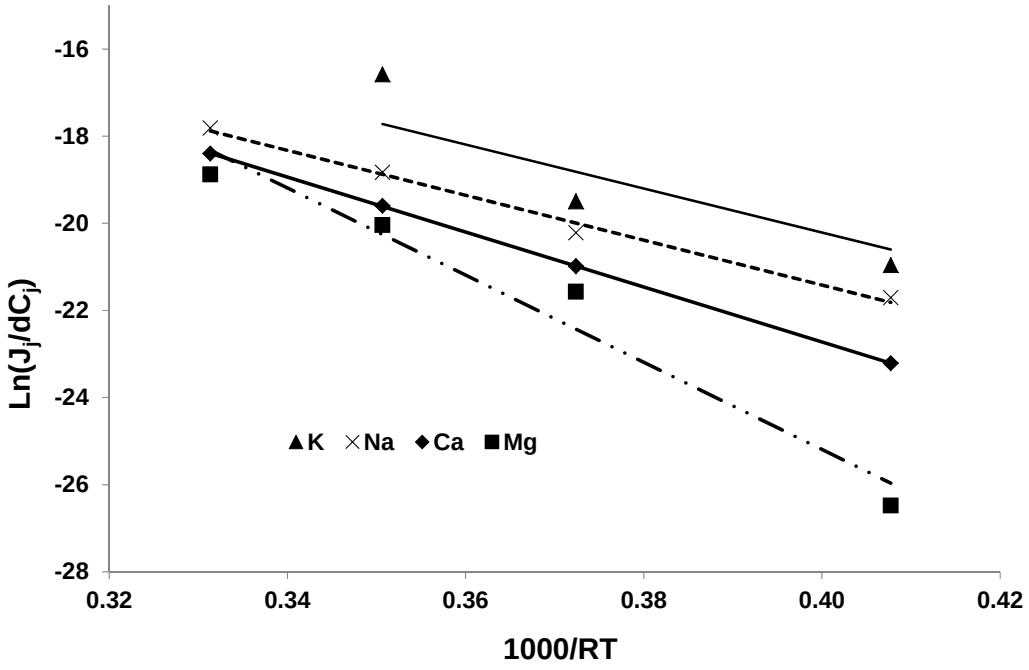

Fig. 7. Arrhenius plots of the overall mass transport coefficients for the cations K^+, Na^+, Ca^{2+}, and Mg^{2+}. 0.3wt% seawater solution (Ca^{2+} 31 mgL^{-1}, Mg^{2+} 100 mgL^{-1}, K^+ 33 mgL^{-1}, Na^+ 948 mgL^{-1}) fed at 700 kPa pressure. J_j ($molm^{-2}h^{-1}$) is the flux of ion *j* (j = K^+, Na^+, Ca^{2+}, or Mg^{2+}) and dC_j is in $molm^{-3}$ where j is the ion; *R* is the universal gas constant (8.315 $LkPamol^{-1}K^{-1}$) and *T* is the system temperature (K).

Although R^2 for K^+ is lower than the other cations because of the effect mentioned above, it is clear that the permeation activation energies for divalent cations Ca^{2+}, and Mg^{2+} are greater than that for monovalent cations K^+, Na^+ (Table 2). This indicates that it requires more energy for these larger ions to diffuse through the zeolite which is sensible considering that they are

larger and probably have a stronger attraction to the zeolite material due to the stronger charge density.

Table 2 The overall activation energies obtained from the Arrhenius plots and correlation coefficient R^2 (Fig. 7) for permeation of the cations K^+, Na^+, Ca^{2+}, and Mg^{2+}.

Ion	Hydrated diameter (nm)	Overall activation energies $\boldsymbol{E_j}$ (kJ/mol)	R^2
K	0.662	50	0.81
Na	0.716	51	0.99
Ca	0.824	63	1.00
Mg	0.856	100	0.96

3.3. SEM

SEM was employed to investigate the morphology of the zeolite membrane before and after long term seawater exposure. Prior to SEM measurements, the desalination tested membrane was rinsed with deionised water to remove weakly adsorbed material (including ions), but was not cleaned too strongly to avoid removing the salts from within the zeolite. Figure 8 shows the SEM images of the top layer of the MFI silicalite membrane. The image (Fig. 8a) of the as-prepared zeolite membrane surface showed typical randomly orientated silicalite crystals. Most of the crystals of silicalite lay disorderly on the surface of the Al_2O_3 support. The top view (Fig. 8b) of the surface of the seawater tested membrane also showed no significant change to the membrane structure after long term seawater exposure. Macrostructure of the membrane remained intact, only some 'loose' deposition of seawater salts on surface was observed after desalination.

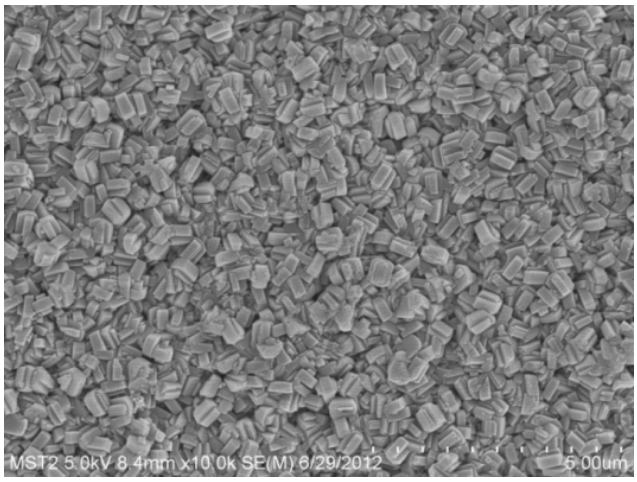

(a)

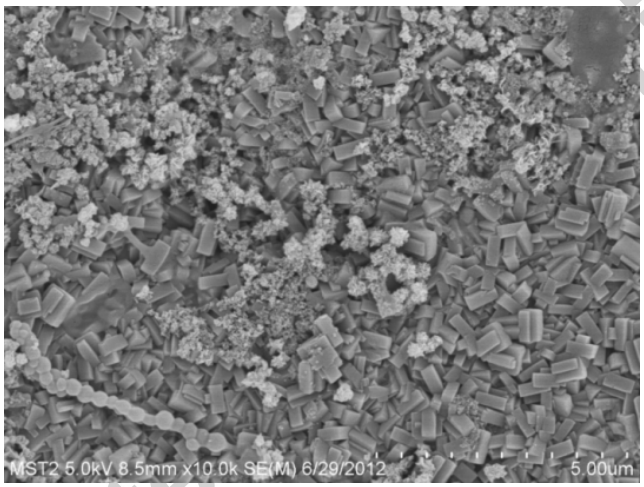

(b)

Fig.8. SEM images on the surface of the zeolite membrane: (a) the original; (b) after long term seawater desalination.

Elemental analysis was also conducted by EDS on both surface and cross-section of the original and desalination tested membrane to determine elemental changes after long term seawater exposure. As shown in Table 3, K^+ and Na^+ were detected on the surface of original zeolite membrane by EDS scanning. This confirms the results obtained from ICP-OES analysis for the permeate samples from the initial pure water testing on the zeolite membrane (Fig. 3). As mentioned earlier in section 3.1, Na^+ and K^+ impurities are from the precursor for membrane synthesis. Comparing the seawater exposed membrane, we see an overall reduction in elements corresponding to the zeolite material (silicon and oxygen) such that the sea salts were making up a larger proportion of the material. Looking more closely, after

seawater treatment there was a decrease in K^+ but Mg^{2+} and Ca^{2+} were detected on the zeolite membrane. The presence of Mg^{2+} and Ca^{2+} coupled with the visible material on the exposed membrane would suggest that some scaling has occurred, however the anion involved is not clear. While sulphate is a strong possibility, carbonate and hydroxide may also be possible. This in turn makes it difficult to determine if the scale is a result of the long exposure time or if it is a result of the higher temperatures used. Regardless, the decrease in presence of potassium also suggests an ion exchange process is occurring. With the increasing concentrations of species limited to Mg^{2+} and Ca^{2+}, this would be the most likely ions exchanged.

Table 3 EDS measured element contents on the zeolite membrane surface before and after 180 day desalination test

Element	Weight percentage before desalination	Weight percentage after desalination
O	46.01	42.94
Na	0.20	0.23
Mg	-	0.11
Al	37.16	31.82
Si	16.32	11.13
Cl	-	0.02
K	0.32	0.03
Ca	-	0.10
Total	100	100

It should be noted that the EDS measured weight percentage of Mg^{2+} (0.11wt%) and Ca^{2+} (0.1wt%) after desalination (Table 3) may have relatively larger measurement errors when compared to that for the elements (e.g. O, Si, Al) with a high concentration. For SEM-EDS, with decreasing concentration, statistical errors and uncertainties in background corrections become dominant. The theoretical detection limits in SEM-EDS measurements are about 0.08wt% [57]. Typical detection limits for EDS are about 0.1% [58]. We should point out here that the membrane was subjected to deionised water permeation after seawater testing. Therefore the detection of ions after seawater and deionised water permeation is a good

indicator that the ions were tightly bound into the zeolite. Therefore it seems that divalent ions are strongly bound into the intercrystalline pores (micro- and mesopores) of zeolite as they have a stronger charge density and are physically larger than monovalent ions. This supports the theory above that temperature alters the structure to facilitate irreversible entrance of divalents into the structure. K^+ was found to be depleted from the material presumably due to the deionised water permeation which supports this theory. Na^+ however remained unchanged and because we have identified that K^+ and Na^+ uniquely enter the zeolite cage (while divalents cannot) [25, 26], it sees that Na^+ preferred to remain in the zeolite cage due to the strong charges within the zeolite structure.

A significant amount of aluminium was also detected on the surface of both original and seawater tested zeolite membrane, suggesting that Al might have incorporated into the zeolite material and/or the zeolite could have grown within the Al_2O_3 substrate. The Al_2O_3-supported MFI membranes are generally not Al free in their frameworks despite of the use of Al-free synthesis solutions during the membrane preparation [7]. Al can incorporate into the zeolite framework due to the dissolution of the Al_2O_3 surface in the high concentration of NaOH synthesis solution and solid-state diffusion of Al^{3+} during calcinations [40]. It is known that the penetration depth of the EDS is 0.5–5 μm [59], but the thickness of the zeolite membranes synthesised by the in-situ method is reported to be ~3 μm [6, 7]. Therefore, EDS could also measure aluminium from the substrate.

3.4. Gas permeation

Gas permeation was used to evaluate the intactness of the zeolite membrane. The permeation of single gas (He or N_2) measured for the original and seawater tested zeolite membrane is shown in Table 4. The gas permeation results for the bare α-Al_2O_3 support are also included in Table 4 for comparison. To release adsorbed water (water molecules can occupy the tight micropore spaces of the zeolite structure), gas permeation test was carried out at 120 °C.

It can be seen from Table 4 that the permeance of He and N_2 measured for the original zeolite membrane was significantly smaller than that of the Al_2O_3 substrate (~34-fold smaller for He and ~24-fold smaller for N_2), confirming that a zeolite layer was formed on the surface of the support. The permeance of He measured for the MFI zeolite membrane

prepared (in-situ method) in this study was smaller than that reported in literature [60] for the MFI zeolite membranes prepared by the seeded secondary growth. This is likely to be due to the different materials (e.g. pore size of the Al_2O_3 substrate) and synthesis conditions (e.g. in-situ or seeded secondary growth) performed within different laboratories. The membrane prepared in this work could be slightly thicker than those in literature [60]. The high resistance of the MFI zeolite membrane prepared in this work may explain partly the low water flux as discussed in Section 3.1. The MFI zeolite membrane [43] prepared in our laboratory by the seeded secondary growth showed a similar level of He permeance to that in literature [60].

Table 4 He and N_2 gas permeation testing on the zeolite membrane at 120 °C before and after desalination

Membrane condition	Permeance of He ($\times 10^{-10}$ molm^{-2}s^{-1}Pa^{-1})	Permeance of N_2 ($\times 10^{-10}$ molm^{-2}s^{-1}Pa^{-1})	He/N_2
α-Al_2O_3 support	6300	4400	1.4
Original	185	180	1.1
After desalination	2.5	0.72	3.5

After desalination testing, a significant decrease in gas permeation on the zeolite membrane was observed, indicating that the membrane was still intact after long term exposure to seawater ion complexes under different conditions. This is in good agreement with the observation from SEM (Fig. 8) showing an intact membrane, and the ion rejection results (Fig. 4) where salt rejections remained reasonably high (>60%) and no size cut off observed. However compared to the initial ion rejection results of >90%, it would seem apparent that some non-selective defects emerged that led to the uniform drop in rejection of all ions at the end of the test (Fig. 4). But this does not correlate with the gas permeation data where flux decreases and selectivity increase would indicate a better desalination membrane. It seems that the membrane experienced a disproportionate loss towards the larger pores of the membrane, which is mainly caused by the filling of the divalent ions into the grain boundaries [25]. So while they infiltrate the zeolite and open the pores thus reducing overall salt rejection, in gas permeation, they are dry and immobile, and instead block the pores to give a lower flux and high selectivity for small molecule gases. The kinetic diameter of He is

0.26 nm and N_2 is 0.36 nm, so since the zeolite has a larger intrinsic pore size (0.56 nm) than these gases it seems highly likely that the reason why gas diffusion was inhibited was because of blocking by adsorbed cations as observed in Table 3. It is also worth pointing out that the He/N_2 selectivity of 3.5 is larger than the Knudsen model value of 2.6 suggesting even the zeolitic pores are sufficiently blocked to allow size selective diffusion of He over N_2 within the MFI intrinsic pores. The finding that ions block pores via this membrane diffusion study aligns with our materials investigation of the influence of ions on MFI-structures [25, 26]. As discussed earlier, it appears temperature accelerated this effect.

4. Conclusions

In the current work, long term desalination through a α-Al_2O_3 supported MFI-type zeolite membrane synthesised by the direct *in-situ* crystallisation method was investigated for a seawater solution (0.3wt% TDS) under a pressure of 700 kPa and at increased temperatures. High rejection (>93%) of the major seawater ions (Ca^{2+}, Mg^{2+} and Na^{+}) was achieved at an operating pressure of 700 kPa and room temperature by the zeolite membrane. With increasing temperature, permeation flux of the zeolite membrane increased but ion rejection decreased. XRD and SEM measurements confirmed the formation of randomly orientated MFI-type silicalite membrane film on the surface of α-Al_2O_3 support, but showed no changes in structure after long term exposure of the membrane to seawater solution. Temperature may have caused accelerated ion diffusion, alterations in the zeolite structure and electrical double layer, and also the hydration diameter of ions, all contributing to penetration of divalent cations that explains why rejections did not increase to their original values when temperature was reduced. The results obtained in this study also confirmed that a nearly perfect rejection of ions including Na^{+} on a real MFI-type zeolite membrane at low temperature is achievable, which has potential application for conventional reverse osmosis desalination. But the ion selective behaviour as a function of temperature may be useful for tuneable ion separation applications.

Acknowledgments

The financial support provided by the Australian Research Council (ARC) through a Discovery Project (DP0986192) is gratefully acknowledged.

References

[1] NRC, Review of the Desalination and Water Purification Technology Roadmap, The National Academic Press, Washington, DC, USA, 2004.

[2] M. Duke, J. O'Brien-Abraham, N. Milne, B. Zhu, Y. S. Lin, J. C. Diniz da Costa, Seawater desalination performance of MFI type membranes made by secondary growth, Separation and Purification Technology. 68(2009) 343-350.

[3] C. H. Cho, K. Y. Oh, S. K. Kim, J. G. Yeo, P. Sharma, Pervaporative seawater desalination using NaA zeolite membrane: Mechanisms of high water flux and high salt rejection, Journal of Membrane Science. 371(2011) 226-238.

[4] W. B. Samuel de Lint, T. Zivkovic, N. E. Benes, H. J. M. Bouwmeester, D. H. A. Blank, Electrolyte retention of supported bi-layered nanofiltration membranes, Journal of Membrane Science. 277(2006) 18-27.

[5] R. Xu, J. Wang, M. Kanezashi, T. Yoshioka, T. Tsuru, Development of robust organosilica membranes for reverse osmosis, Langmuir. 27(2011) 13996-13999.

[6] L. X. Li, J. H. Dong, T. M. Nenoff, R. Lee, Desalination by reverse osmosis using MFI zeolite membranes, Journal of Membrane Science. 243(2004) 401-404.

[7] L. X. Li, J. H. Dong, T. M. Nenoff, R. Lee, Reverse osmosis of ionic aqueous solutions on a MFI zeolite membrane, Desalination. 170(2004) 309-316.

[8] L. X. Li, J. H. Dong, T. M. Nenoff, Transport of water and alkali metal ions through MFI zeolite membranes during reverse osmosis, Separation and Purification Technology. 53(2007) 42-48.

[9] M. Kazemimoghadam, T. Mohammadi, Synthesis of MFI zeolite membranes for water desalination, Desalination. 206(2007) 547-553.

[10] J. Lin, S. Murad, A computer simulation study of the separation of aqueous solutions using thin zeolite membranes, Molecular Physics. 99(2001) 1175-1181.

[11] Y. Deng, C. Deng, D. Qi, C. Liu, J. Liu, X. Zhang, D. Zhao, Synthesis of Core/Shell Colloidal Magnetic Zeolite Microspheres for the Immobilization of Trypsin, Advanced Materials. 21(2009) 1377-1382.

[12] D. J. Doocey, P. N. Sharratt, C. S. Cundy, R. J. Plaisted, Zeolite-Mediated Advanced Oxidation of Model Chlorinated Phenolic Aqueous Waste: Part 2: Solid Phase Catalysis, Process Safety and Environmental Protection. 82(2004) 359-364.

[13] W. Wang, M. Zhou, Q. Mao, J. Yue, X. Wang, Novel NaY zeolite-supported nanoscale zero-valent iron as an efficient heterogeneous Fenton catalyst, Catalysis Communications. 11(2010) 937-941.

[14] E. E. McLeary, J. C. Jansen, F. Kapteijn, Zeolite based films, membranes and membrane reactors: Progress and prospects, Microporous and Mesoporous Materials. 90(2006) 198-220.

[15] S. Li, X. Wang, D. Beving, Z. Chen, Yan, Molecular Sieving in a Nanoporous b-Oriented Pure-Silica-Zeolite MFI Monocrystal Film, Journal of the American Chemical Society. 126(2004) 4122-4123.

[16] S. Murad, K. Oder, J. Lin, Molecular simulation of osmosis, reverse osmosis, and electro-osmosis in aqueous and methanolic electrolyte solutions, Molecular Physics. 95(1998) 401-408.

[17] E. R. Nightingale Jr., Phenomenological theory of ion solvation. Effective radii of hydrated ions, The Journal of Physical Chemistry. 63(1959) 1381-1387.

[18] X. Lin, J. L. Falconer, R. D. Noble, Parallel Pathways for Transport in ZSM-5 Zeolite Membranes, Chemistry of Materials. 10(1998) 3716-3723.

[19] U. Illgen, R. Schäfer, M. Noack, P. Kölsch, A. Kühnle, J. Caro, Membrane supported catalytic dehydrogenation of iso-butane using an MFI zeolite membrane reactor, Catalysis Communications. 2(2001) 339-345.

[20] M. Noack, P. Kölsch, A. Dittmar, M. Stöhr, G. Georgi, M. Schneider, U. Dingerdissen, A. Feldhoff, J. Caro, Proof of the ISS-concept for LTA and FAU membranes and their characterization by extended gas permeation studies, Microporous and Mesoporous Materials. 102(2007) 1-20.

[21] M. Noack, M. Schneider, A. Dittmar, G. Georgi, J. Caro, The change of the unit cell dimension of different zeolite types by heating and its influence on supported membrane layers, Microporous and Mesoporous Materials. 117(2009) 10-21.

[22] D. S. Bhange, V. Ramaswamy, Negative thermal expansion in silicalite-1 and zirconium silicalite-1 having MFI structure, Materials Research Bulletin. 41(2006) 1392-1402.

[23] M. Lassinantti Gualtieri, A. F. Gualtieri, J. Hedlund, The influence of heating rate on template removal in silicalite-1: An in situ HT-XRPD study, Microporous and Mesoporous Materials. 89(2006) 1-8.

[24] M. Lassinantti Gualtieri, C. Andersson, F. Jareman, J. Hedlund, A. F. Gualtieri, M. Leoni, C. Meneghini, Crack formation in α-alumina supported MFI zeolite membranes

studied by in situ high temperature synchrotron powder diffraction, Journal of Membrane Science. 290(2007) 95-104.

[25] B. Zhu, L. Zou, C. M. Doherty, A. J. Hill, Y. S. Lin, X. R. Hu, H. T. Wang, M. Duke, Investigation of the effects of ion and water interaction on structure and chemistry of silicalite MFI type zeolite for its potential use as a seawater desalination membrane, Journal of Materials Chemistry. 20(2010) 4675 - 4683.

[26] B. Zhu, C. M. Doherty, X. Hu, A. J. Hill, L. Zou, Y. S. Lin, M. Duke, Designing hierarchical porous features of ZSM-5 zeolites via Si/Al ratio and their dynamic behavior in seawater ion complexes, Microporous and Mesoporous Materials. 173(2013) 78-85.

[27] M. Noack, P. Kölsch, V. Seefeld, P. Toussaint, G. Georgi, J. Caro, Influence of the Si/Al-ratio on the permeation properties of MFI-membranes, Microporous and Mesoporous Materials. 79(2005) 329-337.

[28] M. Noack, P. Kölsch, A. Dittmar, M. Stöhr, G. Georgi, R. Eckelt, J. Caro, Effect of crystal intergrowth supporting substances (ISS) on the permeation properties of MFI membranes with enhanced Al-content, Microporous and Mesoporous Materials. 97(2006) 88-96.

[29] M. Drobek, C. Yacou, J. Motuzas, A. Julbe, L. Ding, J. C. Diniz da Costa, Long term pervaporation desalination of tubular MFI zeolite membranes, Journal of Membrane Science. 415–416(2012) 816-823.

[30] S. J. Tao, Positronium annihilation in molecular substances (liquids and solids), J. Chem. Phys. 56(1972) 5499-5510.

[31] M. Eldrup, D. Lightbody, J. N. Sherwood, The temperature dependence of positron lifetimes in solid pivalic acid, Chemical Physics. 63(1981) 51-58.

[32] T. L. Dull, W. E. Frieze, D. W. Gidley, J. N. Sun, A. F. Yee, Determination of Pore Size in Mesoporous Thin Films from the Annihilation Lifetime of Positronium, The Journal of Physical Chemistry B. 105(2001) 4657-4662.

[33] T. Humplik, J. Lee, S. C. O'Hern, B. A. Fellman, M. A. Baig, S. F. Hassan, M. A. Atieh, F. Rahman, T. Laoui, R. Karnik, E. N. Wang, Nanostructured materials for water desalination, Nanotechnology. 22(2011) 292001.

[34] [cited 2013 19 February]; Available from: http://www.csmfilter.com/csm/upload/TechManual/Types.pdf.

[35] FILMTEC™ Reverse Osmosis Membranes Technical Manual, The Dow Chemical Company ("Dow"), Form No. 609-00071-1009,

[36] V. Eroshenko, R.-C. Regis, M. Soulard, J. Patarin, Energetics: A New Field of Applications for Hydrophobic Zeolites, Journal of the American Chemical Society. 123(2001) 8129-8130.

[37] N. Desbiens, A. Boutin, I. Demachy, Water Condensation in Hydrophobic Silicalite-1 Zeolite: A Molecular Simulation Study, The Journal of Physical Chemistry B. 109(2005) 24071-24076.

[38] M. Trzpit, M. Soulard, J. Patarin, N. Desbiens, F. Cailliez, A. Boutin, I. Demachy, A. H. Fuchs, The Effect of Local Defects on Water Adsorption in Silicalite-1 Zeolite: A Joint Experimental and Molecular Simulation Study, Langmuir. 23(2007) 10131-10139.

[39] F. Cailliez, G. Stirnemann, A. Boutin, I. Demachy, A. H. Fuchs, Does Water Condense in Hydrophobic Cavities? A Molecular Simulation Study of Hydration in Heterogeneous Nanopores, The Journal of Physical Chemistry C. 112(2008) 10435-10445.

[40] J. Dong, K. Wegner, Y. S. Lin, Synthesis of submicron polycrystalline MFI zeolite films on porous ceramic supports, Journal of Membrane Science. 148(1998) 233-241.

[41] M. Kanezashi, J. O'Brien, Y. S. Lin, Template-free synthesis of MFI-type zeolite membranes: Permeation characteristics and thermal stability improvement of membrane structure, Journal of Membrane Science. 286(2006) 213-222.

[42] I. Kumakiri, T. Yamaguchi, S.-i. Nakao, Application of a zeolite A membrane to reverse osmosis process, Journal of Chemical Engineering of Japan. 33(2000) 333-336.

[43] B. Zhu, J. H. Kim, Y.-h. Na, I.-S. Moon, G. Connor, S. Maeda, G. Morris, S. Gray, M. Duke, Temperature and pressure effects of desalination using a MFI-type zeolite membrane, Membranes. 3(2013) 155-168.

[44] United States Environmental Protection Agency, Membrane Filtration Guidance Manual, Diane Publishing, Darby, PA, 2003.

[45] Y. Liu, X. Chen, High permeability and salt rejection reverse osmosis by a zeolite nano-membrane, Physical Chemistry Chemical Physics. 15(2013) 6817-6824.

[46] L. Li, N. Liu, B. McPherson, R. Lee, Enhanced Water Permeation of Reverse Osmosis through MFI-Type Zeolite Membranes with High Aluminum Contents, Industrial & Engineering Chemistry Research. 46(2007) 1584-1589.

[47] T. C. Bowen, H. Kalipcilar, J. L. Falconer, R. D. Noble, Pervaporation of organic/water mixtures through B-ZSM-5 zeolite membranes on monolith supports, Journal of Membrane Science. 215(2003) 235-247.

[48] G. Bellussi, V. Fattore, Isomorphous substitution in zeolites: a route for the preparation of novel catalysts, in: L. Kubelková, B. Wichterlová, P.A. Jacobs, N.I. Jaeger (G. Bellussi, V.

Fattores), Zeolite Chemistry and Catalysis (Studies in Surface Science and Catalysis), Elsevier, Amsterdam, 1991, pp. 82.

[49] M. Y. Kiriukhin, K. D. Collins, Dynamic hydration numbers for biologically important ions, Biophysical Chemistry. 99(2002) 155-168.

[50] M. Pavlov, P. E. M. Siegbahn, M. Sandström, Hydration of beryllium, magnesium, calcium, and zinc ions using density functional theory, Journal of Physical Chemistry A. 102(1998) 219-228.

[51] N. Liu, L. Li, B. McPherson, R. Lee, Removal of organics from produced water by reverse osmosis using MFI-type zeolite membranes, Journal of Membrane Science. 325(2008) 357-361.

[52] U. Merten, Desalination by pressure osmosis, Desalination. 1(1966) 297-310.

[53] M. Chaplin. *Water Structure and Science: Ion Hydration and Aqueous Solutions of Salts*. 2012 [cited 2013 21 February]; Available from: http://www.lsbu.ac.uk/water/ions.html.

[54] C. A. Fyfe, H. Strobl, G. T. Kokotailo, G. J. Kennedy, G. E. Barlow, Ultra-high-resolution /sup 29/Si solid-state MAS NMR investigation of sorbate and temperature-induced changes in the lattice structure of zeolite ZSM-5, Journal of the American Chemical Society 110(1988) 3373-3380.

[55] E. L. Wu, S. L. Lawton, D. H. Olson, A. C. Rohrman, G. T. Kokotailo, ZSM-5-type materials. Factors affecting crystal symmetry, The Journal of Physical Chemistry. 83(1979) 2777-2781.

[56] A. J. Bard, L. R. Faulkner, Electrochemical Methods: Fundamentals and Applications 2nd ed., John Wiley and Sons, Hoboken, USA, 2001.

[57] S. J. B. Reed, Electron Microbe Analysis and Scanning Electron Microscopy in Geology, Cambridge University Press, Cambridge, 1996.

[58] *Introduction to Energy Dispersive X-ray Spectrometry (EDS)*. [cited 2013 05 March]; Available from: http://micron.ucr.edu/public/manuals/EDS-intro.pdf.

[59] Electronic Device Failure Analysis Society (EDFAS), Microelectronic Failure Analysis: Desk Reference : 2002 Supplement, ASM International, Materials Park, OH, 2002.

[60] J. O'Brien-Abraham, M. Kanezashi, Y. S. Lin, A comparative study on permeation and mechanical properties of random and oriented MFI-type zeolite membranes, Microporous and Mesoporous Materials. 105(2007) 140-148.

Research highlights:

- 180 day stability of MFI-type zeolite membrane for seawater desalination was confirmed.
- The membrane achieved a high rejection (>93%) for the major seawater ions including Na^+.
- Increasing the temperature decreased the ion rejection and increased the permeation flux.
- Larger ions Ca^{2+} and Mg^{2+} were less responsive to temperature than smaller ions Na^+ and K^+.
- Ions infiltrate the zeolite material and alter its size selective property.